J|A|C|S
ARTICLES
Published on Web 08/29/2006

X-ray Diffraction Area Mapping of Preferred Orientation and Phase Change in TiO_2 Thin Films Deposited by Chemical Vapor Deposition

Geoffrey Hyett, Mark Green, and Ivan P. Parkin*

Contribution from Christopher Ingold Laboratories, University College London, 20 Gordon Street, London WC1H 0AJ, United Kingdom

Received April 20, 2006; Revised Manuscript Received July 12, 2006; E-mail: i.p.parkin@ucl.ac.uk

Abstract: This paper reports on an investigation into the formation of TiO_2 thin films, whereby X-ray diffraction is used to map systematic changes in preferred orientation and phase observed throughout the films. The key to this strategy is the recording of X-ray diffraction patterns of specific and isolated areas of a substrate, ensuring this specificity by the use of a small X-ray sample illumination area (approximately 3−5 mm^2). A map of the variation in film composition can then be built up by recording such diffraction patterns at regular intervals over the whole substrate. Two titania films will be presented, grown using atmospheric pressure chemical vapor deposition, at 450 and 600 °C, from $TiCl_4$ and ethyl-acetate precursors. The film grown at 450 °C showed a systematic change in preferred orientation, while the film grown at 600 °C was composed of a mixture of the rutile and anatase phases of TiO_2 with the ratio of these phases altering with position on the substrate. The results of physical property measurements and electron microscopy carried out on the films are also reported, conducted at locations identified by the X-ray diffraction mapping procedure as having different compositions, and hence different physical responses. We found that the photocatalytic activity and hydrophobicity were dependent on the rutile:anatase ratio at any given location on the film.

Introduction

Low-angle X-ray diffraction is a widely used technique for the investigation of thin films of solid-state compounds. This is because it is both convenient and effective for the identification of crystalline phases. In the vast majority of thin film investigations, however, the diffraction is conducted only on a small number of sections, or indeed a single section, of the total area of the coated substrate; the coating is then assumed to be effectively uniform and the results from these small sections considered as being valid for the whole of the coated substrate.[1,2] It is also common that the X-ray illumination areas used in these diffraction experiments are large (1−2 cm^2), such that the measured patterns show the average composition for the studied area, and any information about subtle localized change in composition is lost.

The strategy outlined in this paper is to use a much smaller X-ray sample illumination area of 3−5 mm^2, such that each X-ray diffraction pattern can be considered as representing a localized area of the substrate, and to record an array of these diffraction patterns at regular intervals across the substrate, allowing a map of the film composition to be generated.

Area mapping diffraction experiments have been previously used to produce three-dimensional maps of samples, using the diffraction of neutrons or synchrotron sourced X-rays. These techniques are routinely used to analyze bulk engineering or archaeological materials for varying composition, texture, and strain.[3−5] Such tests are conducted so as to determine, nondestructively, the composition and character of the samples, and use the penetrating nature of these radiation sources, as compared to laboratory generated X-rays, combined with the small illumination volumes that can be obtained (for example, in energy dispersive instruments) to allow the compositional changes throughout a bulk macroscopic sample to be accurately mapped.

The use of diffraction mapping in 2D films, as described in this paper, is, however, much less common. One reason for the under-use of X-ray mapping in two-dimensional films is that until recently such experiments have not been achievable on reasonable time scales without the use of synchrotron sources of radiation. Previous authors that have used such a strategy have done so predominantly to investigate epitaxial films grown on silicon substrates.[6,7] Such a technique is generic and can be applied to virtually any thin film. In this paper, we present what

(1) Blackman, C.; Carmalt, C. J.; Parkin, I. P.; O'Neill, S.; Apostolico, L.; Molloy, K. C.; Rushworth, S. *Chem. Mater.* **2002**, *14*, 3167−3173.
(2) Seifried, S.; Winterer, M.; Hahn, H. *Chem. Vap. Deposition* **2000**, *6*, 239−244.
(3) Ganguly, S.; Fitzpatrick, M. E.; Edwards, L. *Metall. Mater. Trans. A* **2006**, *37A*, 411−420.
(4) Sinclair, R.; Preuss, M.; Withers, P. J. *Mater. Sci. Technol.* **2005**, *21*, 27−34.
(5) Poulsen, H. F. *Appl. Phys. A* **2002**, *74*, S1673−S1675, Part 2, Suppl. S.
(6) Zaumseil, P.; Lafford, T. A.; Taylor, M. *J. Phys. D: Appl. Phys.* **2001**, *34*, A52−A56.
(7) Takeuchi, I.; Long, C. J.; Famodu, O. O.; Murakami, M.; Hattrick-Simpers, J.; Rubloff, G. W.; Stukowski, M.; Rajan, K. *Rev. Sci. Instrum.* **2005**, *76*, 062223/1−062223/8.

we believe is the first time that it has been used to measure phase and texture changes in titania films, on laboratory-based instruments.

The work in this paper shows the benefit of using an X-ray area map and a deposition system that has a built-in asymmetry (such as temperature or reactant concentration gradients) that allows for a combinatorial CVD approach. In effect, over 150 separate spots can be analyzed, each with a slightly different set of deposition conditions. This allows a significant gain in time and cost as over 150 CVD experiments are effectively replicated in a single measurement. Additionally, recent developments in powder diffractometer technology have now made it possible to record the necessary number of diffraction patterns to map a substrate in a 24 h period. To record a similar number of patterns on a more traditional instrument, such as a Siemens D5000 with a PSD, would require almost 3 months of continuous machine operation. Hence, we have demonstrated that such diffraction mapping is now possible using a laboratory source on a reasonable time scale.

To demonstrate the efficacy of this method of X-ray diffraction pattern mapping for compositional analysis, two thin films of TiO_2 on a glass substrate were produced and mapped. Titania was chosen for the test films because it is a relatively simple, yet scientifically interesting, system with several accessible phases and one that has been the focus of many former publications, so its formation and properties are well understood. Such films have been formerly synthesized using physical vapor deposition,[8] atmospheric pressure chemical vapor deposition,[9,10] low-pressure CVD,[11] MOCVD,[12] and sol−gel calcination[13] routes.

The reason for this extensive research interest in the field of TiO_2 films (710 published papers in 2004, and 757 in 2005[14]) lies in the chemical and physical properties that such films exhibit, and the commercial exploitation of these properties in self-cleaning coatings. TiO_2 films have been found to be photocatalytic and have photoactivated superhydrophilicity, and it is these properties that make it highly suitable for self-cleaning glass coatings (e.g., Pilkington Activ, SGG BioClean, and PPG SunClean), as the hydrophilic properties allow greater wetting of the surface to wash off dirt, and the photocatalysis promotes degradation of any organic residue. These coatings were first commercialized in 2001 and now have sales in excess of £100 m per annum.[15] The range of products utilizing titania self-cleaning coatings also includes self-cleaning ceramic tiles, sanitaryware, and deodorizing products.[16]

The photocatalytic ability of semiconducting TiO_2 films is activated when they are exposed to photons with energy greater than that of the TiO_2 band gap. Electrons are promoted to the conduction band by the photon, producing an electron−hole pair, which can then migrate to the surface and promote redox reactions occurring on the surface of the film,[17,18] such as the atmospheric oxidation to CO_2 and H_2O of organic residues (i.e., dirt).

In commercial self-cleaning coatings, the anatase phase of TiO_2 has been most utilized.[18] This is a white semiconductor with a band gap of 3.2 eV,[19] a refractive index of 2.55, and a structure comprised of TiO_6 octahedra, which each share four of their edges with four neighboring TiO_6 polyhedra. It is normally the predominant phase formed in atmospheric CVD below 640 °C.[9] The most thermodynamically stable phase of TiO_2 under standard conditions is rutile, the denser phase, with a smaller, indirect band gap of 3 eV,[20] a refractive index of 2.65, and a structure based on edge-sharing chains of TiO_6. In atmospheric pressure CVD, rutile is normally only formed above 640 °C.[21] It has been a matter of considerable debate as to whether pure anatase or mixed anatase−rutile will provide the most effective photocatalyst.[18] For example, samples of Degussa P25 (80% anatase, 20% rutile) are often taken to be the industrial benchmark for an active photocatalyst. Here, we shed light on this debate and show that for thin film samples a pure anatase film gives the best functional properties.

Results and Discussion

A number of films of TiO_2 were grown by atmospheric pressure chemical vapor deposition reaction of $TiCl_4$ and ethyl-acetate, at both 450 and 600 °C, on glass substrates with surface areas of 89 mm × 225 mm. These films were principally analyzed by X-ray diffraction mapping with patterns being recorded every 10 mm in both *x* and *y* directions, to produce a grid of 168 diffraction patterns (21 × 8 spots). For labeling purposes, these were considered as eight strips running parallel to the longest side of the slide, denoted A−H from top to bottom, orientated with the leading edge of the substrate on the right-hand side. Within each strip, the spots were labeled 1−21 in the direction of the gas flow. Of the films produced, two representative samples were selected and investigated in detail. The results of these investigations are presented below.

Titania Film Grown at 450 °C. The thin film of TiO_2 grown on the substrate heated to 450 °C appeared, by visual inspection, to cover the whole glass sheet and was weakly colored at non-normal viewing angles in a series of "rainbow fringes", caused by the varying film thickness across the substrate. The observed colors originate from interference effects of light reflected from the TiO_2/air and TiO_2/glass interfaces. The observed color is dependent on the path length, and this enabled the thickness of the film to be determined. Using this method, we generated a contour map of the film's thickness, which is displayed in Figure 1 along with the spot labeling system. This shows that the film was thickest at the center and decreases in thickness toward the edges. This matches the pattern of temperature variation over the substrate. A cold walled reactor was used, with the substrate heated through a carbon block. The carbon block was itself heated by three internal cartridge heaters. However, as the reactor was not externally heated, the edges of the substrate

(8) DeLoach, J. D.; Scarel, G.; Aita, C. R. *J. Appl. Phys.* **1999**, *85*, 2377−2384.
(9) O'Neill, S. A.; Parkin, I. P.; Clark, R. J. H.; Mills, A.; Elliott, N. *J. Mater. Chem.* **2003**, *13*, 56−60.
(10) O'Neill, S. A.; Clark, R. J. H.; Parkin, I. P.; Elliott, N.; Mills, A. *Chem. Mater.* **2003**, *15*, 46−50.
(11) Rausch, N.; Burte, E. P. *J. Electrochem. Soc.* **1993**, *140*, 145−149.
(12) Shalini, K.; Chandrasekaran, S.; Shivashankar, S. A. *J. Cryst. Growth* **2005**, *284*, 388−395.
(13) Vorotilov, K. A.; Orlova, E. V.; Petrovsky, V. I. *Thin Solid Films* **1992**, *207*, 180−184.
(14) Based on a search of the ACS Chemical Abstracts database for "thin films of TiO_2".
(15) See company websites: www.pilkington.com, www.saint-gobain.co.uk, and www.ppg.com.
(16) Parkin, I. P.; Palgrave, R. G. *J. Mater. Chem.* **2005**, *15*, 1689−1695.
(17) Hagfeldt, A.; Gratzel, M. *Chem. Rev.* **1995**, *95*, 49−68.
(18) Mills, A.; LeHunte, S. *J. Photochem. Photobiol., A* **1997**, *108*, 1−35.
(19) Tang, H.; Berger, H.; Schmid, P. E.; Levy, F.; Burri, G. *Solid State Commun.* **1993**, *87*, 847−850.
(20) Pascual, J.; Camassel, J.; Mathieu, H. *Phys. Rev. B* **1978**, *18*, 5606−5614.
(21) Ghoshtag, R. N.; Noreika, A. J. *J. Electrochem. Soc.* **1970**, *117*, 1310−1314.

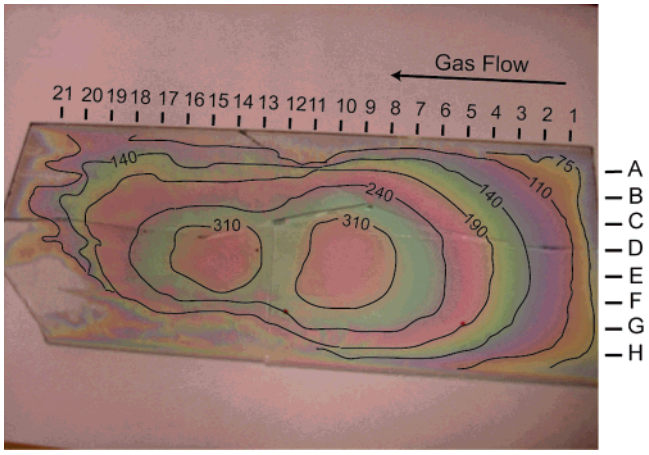

Figure 1. Photograph of the TiO_2 film grown at 450 °C showing the interference fringes, and superimposed with the spot labeling system and film depth contour lines (thickness of film is in nanometers).

were inevitably slightly cooler than the center, a difference of between 15 and 20 °C, dependent on exact location. As the deposited film was thinner at the edges than at the center, following the same pattern as was observed in the temperature variation, it was suggested that film thickness was dependent on the substrate temperature; a higher substrate temperature allowed a thicker film to grow. This indicates that the deposition was surface reaction rate-limited rather than limited by precursor depletion, as in such a case we would observe the TiO_2 becoming consistently thinner along the substrate.

The 168 X-ray diffraction patterns measured across the sample substrate all gave similar diffraction patterns, which could be indexed as the anatase phase of TiO_2 ($I4_1/amdz$, a = 3.78479(7) Å, c = 9.5119(3) Å). The recorded diffraction patterns did not, however, show the same relative peak intensities as those predicted for bulk powder anatase. This was due to preferred orientation of the crystallites. An example strip of the diffraction patterns in which this can be seen, those of the 21 spots in strip C, is shown in Figure 2. A similar range of diffraction patterns was found in all of the other strips. The large hump seen in the background of the patterns centered around approximately $2\theta = 25°$ is caused by diffraction from the amorphous glass substrate, by X-rays that penetrate through the thin film of titania.

The preferred orientation seen in the diffraction patterns of the substrate was not, however, the same for all of the patterns, although the 101 peak was always the most intense. Instead, the patterns could be divided into three groups, based on their relative peak intensity. In the first group, the 112 peak was more intense than the 200 peak (type A), in the second the 112 and 200 were of equivalent intensity (type B), and in the third the 200 was stronger than the 112 (type C). The locations of each type of pattern on the substrate are shown schematically in Figure 3. This shows that type A seemed to predominate on the leading edge side of the substrate, with respect to the direction of the gas flow, to be replaced by type B as the predominant preferred orientation from around 9−14 cm from the leading edge of the substrate. Significantly, the preferred orientation type does not follow the same pattern across the substrate as the film thickness (and hence temperature gradient).

To investigate the preferred orientation more fully, three spots on the substrate, one of each of the identified types, were

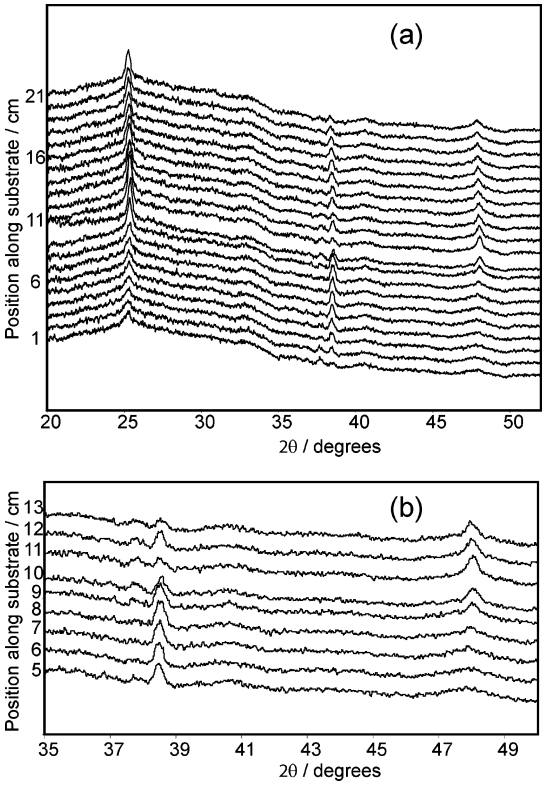

Figure 2. (a) Plot of the diffraction patterns from all 21 spots in "strip C" of the film grown at 450 °C. (b) Highlight of the 112 and 200 peaks in the patterns in strip C between 5 and 13 cm along the substrate, showing the switch in preferred orientation.

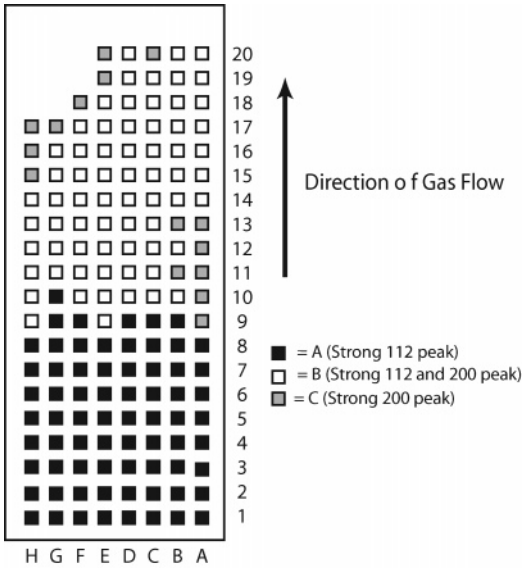

Figure 3. Schematic diagram of the 450 °C film, showing the type of preferred orientation found at each spot.

selected (G5 and G11 and H16), and these spots had their diffraction patterns recorded with much longer exposure times of 1 h to improve the signal-to-noise ratio. These longer scans were then used in a Rietveld refinement where the March−Dollase function was applied to determine the preferred orientation of the crystallites causing the different relative peak intensities.

The refinements found that type A had the crystallites preferentially aligned in the (111) plane with a March coefficient, r, of 0.34 (the r value is a measure of the degree of

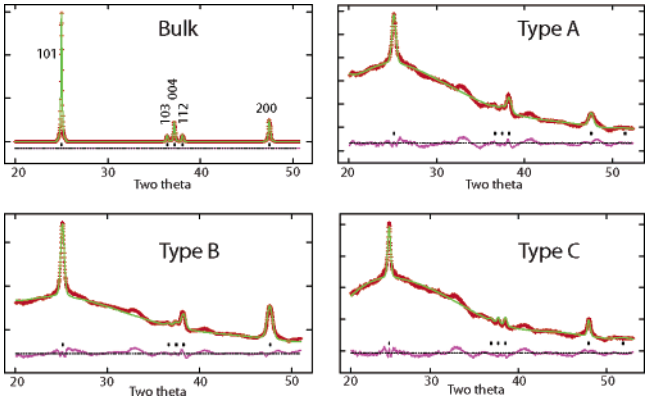

Figure 4. X-ray powder diffraction patterns of the 450 °C film with Rietveld modeling. Red lines are recorded data, and green lines are Rietveld model patterns; difference plots are shown in purple. The large background of ca. 25° 2θ is caused by amorphous scattering from the glass substrate.

preferred orientation; at $r = 1$, the crystallites are arranged randomly and there is no preferred orientation).[22] In type B, the crystallites had to be modeled with a mixture of two types of preferred orientation, 89% in the (111) plane ($r = 0.34$), as found in type A, and 11% in the (100) plane ($r = 0.38$). Type C was also found to have preferred orientation in the (111) plane, the same as type A, although to a lesser extent than that found in type A with $r = 0.51$. The diffraction patterns of these three longer scans along with their refined model patterns are shown in Figure 4. For comparison, an example of the predicted pattern for randomly oriented bulk anatase is also shown in the figure.

Thus, the strategy of X-ray mapping that had been applied to this TiO_2 film has identified that the film is not uniform and that a range of preferred orientations can be found. The X-ray diffraction patterns found that on the leading edge side of the substrate the crystallites were preferentially aligned along the (111) face while further along the substrate (in the type B zone) the (111) preferred orientation is still the dominant orientation, but with some additional crystallites with orientation along the (100) plane. In these films, the substrate is amorphous, and so the preferred orientation is not caused by lattice matching as is found in some epitaxially grown films, and so must be related to the mechanism of deposition.

On the basis of the characterization of the substrate from the X-ray map, physical and optical property tests were conducted on spots with each of the three preferred orientation types. Water contact angle measurements were conducted before and after irradiation with 254 nm UV light, to determine the extent of any photoactivated hydrophilicity; the photocatalytic ability of the films was tested by depositing a layer of stearic acid onto the film, and then exposing the film to UV light, periodically assessing the amount of stearic acid destroyed. Such tests have been previously used to determine the photoactivated properties of TiO_2 films.[23,24]

The results of the water contact angles tests for various sections of the film are shown in Table 1. This shows the TiO_2 film changes from being hydrophobic to hydrophilic after irradiation and that this effect is approximately equal for all of

Table 1. Results of the Contact Angle Tests on TiO_2 Film Grown at 450 °C

type	pre-irradiation	post-irradiation
A	87(7)°	10.6(0.8)°
B	80(7)°	13(1)°
C	73(7)°	7.9(0.5)°
plain glass standard	35(3)°	35{3)°

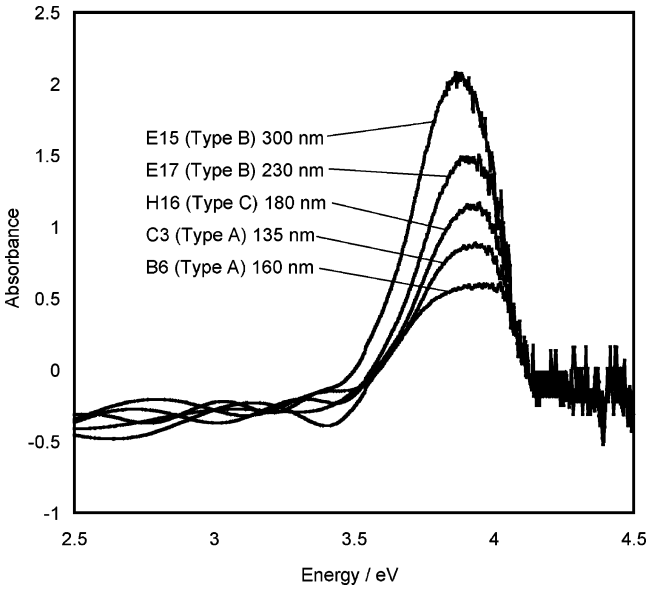

Figure 5. Plot of the UV−vis absorbance spectra of selected spots on the film grown at 450 °C.

the observed preferred orientations; hence, in this system, the preferred orientation does not affect photoactivated hydrophilicity.

The UV absorbance spectra of four of the substrate spots are shown in Figure 5. All of these spectra share the same profile (that of anatase), but with different intensities. The absorbance of the film is proportional to the amount of titania, and thus is proportional to the film thickness (assuming constant film density). The values of the film thickness are shown in the figure key and show a correlation to the intensity of absorbance, with the thickest sections of the film corresponding to the most intense absorption profiles. The UV absorption profiles do not seem to be affected by the preferred orientation of the films.

The stearic acid destruction test results found rates of destruction of stearic acid consistent with first-order kinetics (both first- and zeroth-order kinetics have been previously observed[26]). The first-order rate constants for each of the tested spots are shown in Table 2. These show that the rate of stearic acid destruction is not consistent across the whole film but varies across the five recorded spots. This variation in stearic acid destruction, however, does not seem to depend on the preferred orientation, but again on film thickness. The greatest rate of destruction (such that no stearic acid is detectable after 200 min) is found in spot E15, where the film is approximately 300 nm thick. The slowest film destruction rates are found in spots B6 and C3, which are 135 and 160 nm thick, respectively. This has been observed before[9,25] and can be rationalized, to a first

(22) Dollase, W. A. *J. Appl. Crystallogr.* **1986**, *19*, 267−272, Part 4.
(23) Mills, A.; Elliott, N.; Parkin, I. P.; O'Neill, S. A.; Clark, R. J. *J. Photochem. Photobiol., A* **2002**, *151*, 171−179.
(24) Paz, Y.; Luo, Z.; Rabenberg, L.; Heller, A. *J. Mater. Res.* **1995**, *10*, 2842−2848.
(25) Mills, A.; Lee, S.; Lepre, A.; Parkin, I. P.; O'Neill, S. A. *Photochem. Photobiol. Sci.* **2002**, *1*, 865−868.
(26) Mills, A.; Lepre, A.; Elliott, N.; Bhopal, S.; Parkin, I. P.; O'Neill, S. A. *J. Photochem. Photobiol., A* **2003**, *160*, 213−224.

Table 2. First-Order Rate Constants for the Destruction of Stearic Acid on Spots of TiO_2 Film Grown at 450 °C

spot	B6	E17	E15	C3	H16
preferred orientation type	A	B	B	A	C
film depth	160	230	300	135	180
rate constant/$\times 10^{-3}$ min^{-1}	1.72(4)	3.4(2)	8.4(6)	1.6(1)	3.2(2)

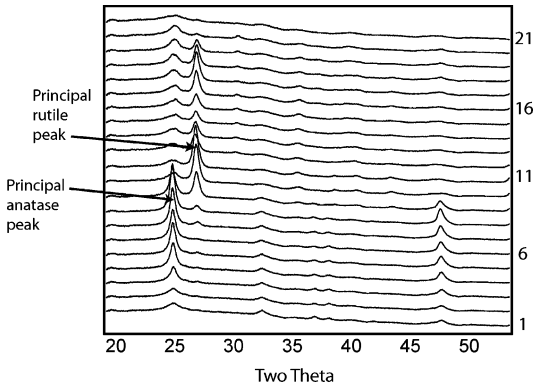

Figure 6. Representation of the X-ray patterns of the 21 spots in "strip B" of the film grown at 600 °C. Both rutile and anatase Bragg peaks can be observed.

approximation, as thicker films tend to be rougher, and therefore have larger surface areas per substrate area. This means that in the thicker films more reaction sites are available, allowing more stearic acid to be catalytically degraded. In commercial films, however, the film thickness is chosen primarily to optimize optical clarity and minimize cost, rather than to maximize photoactivity.

The physical property tests have thus found that the film grown at 450 °C was photocatalytic and becomes superhydrophilic after exposure to UV light. We have been able to conclude that the difference in UV absorption and photocatalytic activity between the spots was dependent on the film thickness, and not the differences in preferred orientation.

Titania Film Grown at 600 °C. The TiO_2 film grown at 600 °C covered the whole of the substrate and had rainbow fringes associated with varying film thickness, but these "contour" lines were found to be closely spaced at the edges of the slide and greater in number than found in the 450 °C film, such that the film thickness, as assessed by color analysis, rapidly increases within 10 mm of the edge of the film to a plateau 520−600 nm thick, which covers the majority of the substrate with a film of consistent thickness. This film was also analyzed using the X-ray mapping technique, again covering 168 spots in an 8 × 21 grid.

The X-ray diffraction patterns recorded on the film supported the visual inspection and found, as was the case for the 450 °C film, the presence of crystalline TiO_2 across the whole of the substrate. In the 600 °C film, however, two different phases of TiO_2 were observed, both rutile and anatase, in varying ratios across the substrate. An example strip of the X-ray patterns, showing the presence of both phases, is depicted in Figure 6. This shows that near the leading edge of the substrate, up to 7 cm in, anatase is by far the predominant phase, with only small amounts of rutile detectable. From 7 cm onward, the phase fraction of rutile increases until it is the dominant phase, although anatase is always still detectable.

Consideration of all of the diffraction patterns found that anatase was the dominant phase, present to some extent in all

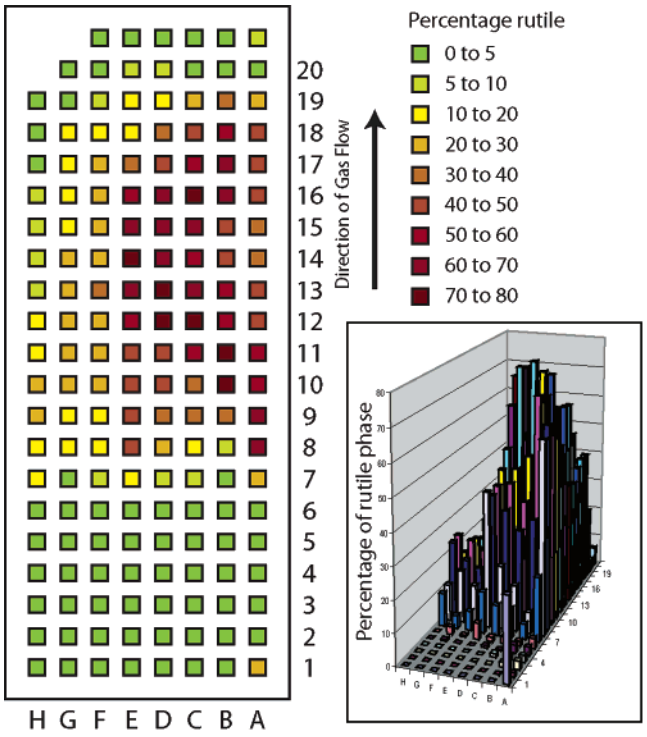

Figure 7. Schematic diagrams of the 600 °C film, showing the fraction of each of the spots composed of rutile.

of the spots, and in some cases the only detectable phase. The rutile phase was found in conjunction with the anatase phase from 8 to 20 cm from the leading edge, mostly as the lesser phase, although in some of the spots it was the dominant phase (for example, at spot B11 seen near the center of Figure 6). To quantify the varying relative phase fraction across the substrate, the X-ray diffraction patterns were modeled as a mixture of anatase and rutile, then refined using the Rietveld method, with phase fraction of rutile being one of the refined parameters. The cell parameters used for modeling anatase were $I4_1/amdz$, a = 3.782 Å, c = 9.504 Å, and for rutile they were $P4_2/mnm$, a = 4.624 Å, c = 2.9836 Å.

The results of the Rietveld analysis are shown in Figure 7, where the percentage of rutile present at each diffraction spot is identified. This allows the concentration of the rutile phase localized in strips A−E, from 10 to 18 cm, to be clearly seen.

The Rietveld refinement also found that both phases show preferred orientation (in the (111) plane in both cases, the predominant preference also found in the 450 °C film), but unlike the film synthesized at lower temperature the preferred orientation did not change significantly across the substrate.

Thus, the X-ray mapping showed that the 600 °C film was not uniform, but composed of a varying ratio of the anatase and rutile phases of TiO_2. To determine the differences in physical and optical properties that these sections might have due to the different phase fractions, four spots with different rutile contents of 0:100, 25:75, 50:50, and 80:20, rutile:anatase,

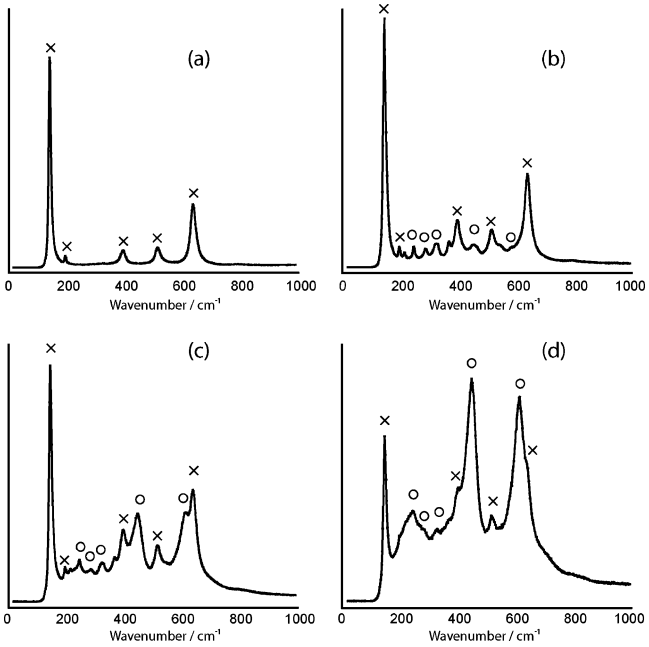

Figure 8. Raman spectra of spots of the TiO_2 film grown at 600 °C. Peaks marked ○ correspond to rutile library pattern peaks, and those marked × correspond to anatase. (a) Spectra of 100% anatase spot. (b) Spectra of 75% anatase, 25% rutile spot. (c) Spectra of 50% anatase, 50% rutile spot. (d) Spectra of 20% anatase, 80% rutile spot.

respectively, were tested using the water contact angle test, stearic acid test, UV spectroscopy, and Raman spectroscopy.

The Raman spectra of the four spots were compared to library patterns of rutile and anatase to determine which of the observed peaks corresponded to which phase.[27] These spectra are reproduced in Figure 8. The spot determined from Rietveld analysis as containing only anatase also displays only anatase peaks in the Raman spectra. The other spots contain Raman peaks corresponding to both rutile and anatase (based on the library patterns), in proportions consistent with the ratios of the two phases determined by the Rietveld analysis. Thus, the recorded Raman spectra provide evidential support for the assignment of the phase compositions made by X-ray diffraction analysis.

The UV absorbance spectra for the four spots are displayed in Figure 9. The spectra show that all four spots have similar absorbance intensities and hence similar thickness, but different absorbance profiles. The 100% anatase spot and 80:20, rutile:anatase spots (based on X-ray diffraction) have UV spectra that match well the previously recorded literature spectra[19] for anatase and rutile, respectively. The anatase-only spot has a sharper absorbance peak than the 80:20 rutile spot, and one that occurs at higher energy, an expected result as the anatase band gap is larger. The 50:50 and 25:75 spots have UV absorbance profiles, which, as would be expected, appear to be superimposed combinations of the anatase and rutile absorption profiles, so these results also support our assignment from X-ray diffraction of the film thickness and composition at these positions on the substrate.

The results of the water contact angle tests are given in Table 3. This table shows a significant difference in the post-irradiative contact angle of the 80% rutile spot as compared to those of

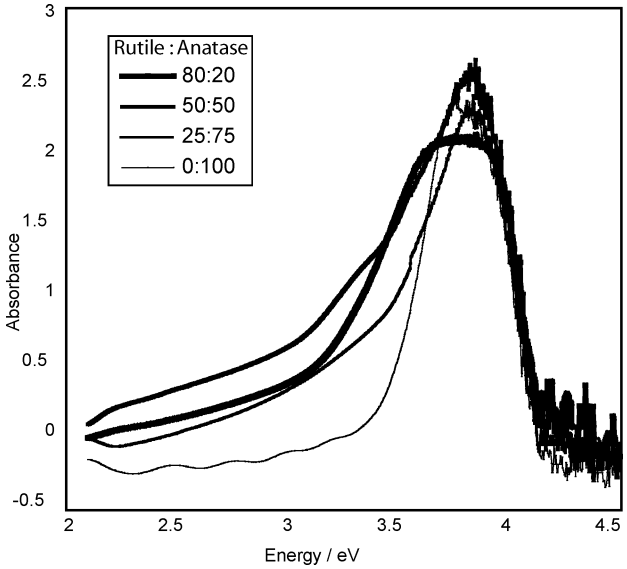

Figure 9. Plot of the UV−vis absorbance spectra of selected spots on the film grown at 600 °C.

Table 3. Results of the Contact Angle Tests on TiO_2 Film Grown at 600 °C

%rutile:anatase	pre-irradiation	post-irradiation
0:100	73(7)°	25(2)°
25:75	65(6)°	13(2)°
50:50	60(6)°	28.4(2)°
80:20	61(6)°	87(8)°
plain glass standard	35(3)°	35(3)°

the low rutile content spots. The spot composed of 80% rutile becomes more hydrophobic upon irradiation, while the spots with significant anatase phase fractions become hydrophilic upon irradiation. Photographs of some of the droplets are shown in Figure 10, which highlight just how extreme the difference in contact angle is between the high rutile content spots and the high anatase content spots of the film.

The stearic acid destruction tests conducted on the 600 °C TiO_2 film show destruction rates consistent with zeroth-order kinetics, found in TiO_2 films when the surface catalytic sites are saturated with stearic acid.[26] The rates of stearic acid degradation found for each of the spots are reported in Table 4, while Figure 11 shows the number of molecules of stearic acid per unit area remaining on the film plotted against the irradiation time. These results show that the photocatalytic strength of the film scales with the proportion of anatase to rutile from 4.6×10^{12} to 8×10^{12} molecules cm^{-2} min^{-1}, with the anatase-only portion of the film having the greatest rate of stearic acid destruction. These are comparable to previous measurements conducted on chemical vapor deposited TiO_2[23] of 4×10^{12} molecules cm^{-2} min^{-1} and of Pilkington Activ[26] glass of 8×10^{12} molecules cm^{-2} min^{-1} (figures adjusted for UV light intensity).

Electron microscope imaging was also carried out on the spots, and these images are shown in Figure 12. These pictures show that in the anatase-only section the film is composed of small particles of approximately 75−100 nm in diameter. The sections containing both rutile and anatase contain both small particles, similar in size and appearance to that found on the anatase-only spot, and also much larger crystallites, approximately 200−300 nm in diameter. This difference in the SEM

(27) Burgio, L.; Clark, R. J. H. *Spectrochim. Acta, Part A* **2001**, *57*, 1491−1521.

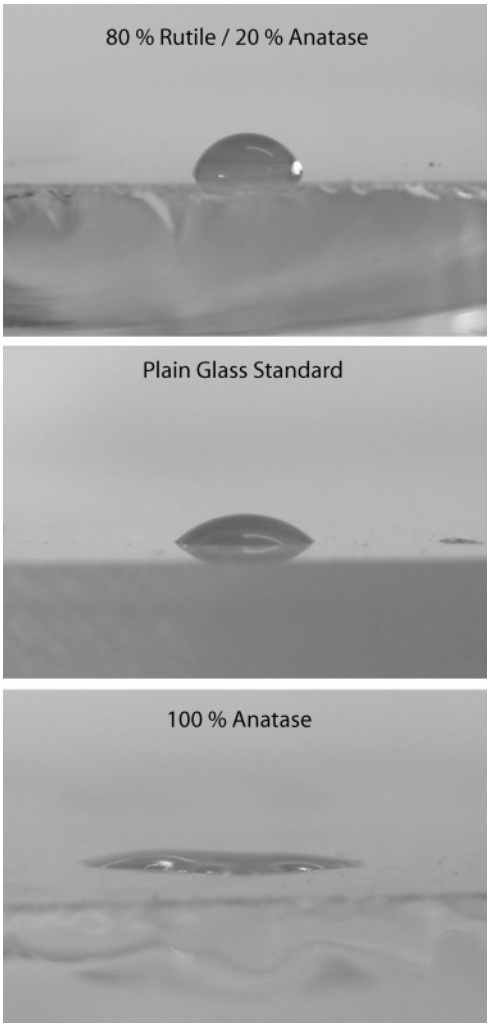

Figure 10. Photographs of water drops on sections of 600 °C film and a plain glass comparison after irradiation with UV light, highlighting the changes in contact angle.

Table 4. Zeroth-Order Rate Constants for the Destruction of Stearic Acid on Various Spots of the 600 °C Film

rutile:anatase	0:100	25:75	50:50	80:20
rate constant/$\times 10^{12}$ molecules cm^{-2} min^{-1} 10^{12}	7.9(3)	6.0(2)	5.2(2)	4.6(3)

images makes it tempting to suggest that the smaller crystallites are composed of anatase and that the larger crystallites are composed of rutile. Evidence to support this assignment is found in the X-ray diffraction patterns, where the anatase peaks have a larger full width at half-maximum (fwhm) than the rutile peaks (0.76° vs 0.48° in 2θ); such peak broadening is associated with small crystallite size. The Scherrer equation allows an estimation of particle size based on the peak broadening, and this analysis gave values for the particle size of anatase as 14(1) and 47(1) nm for the particle size of rutile. So the X-ray diffraction peak broadening does support the assignment of the particles seen in the SEM, but further evidence would be required to definitively prove the assignment.

The SEM images also suggest that the morphology could aid in explaining the photocatalysis results. The images clearly show that the rutile-containing spots have much rougher surfaces than the anatase-only spot. So if the relative rates of photocatalysis of the different spots were dependent only on the surface

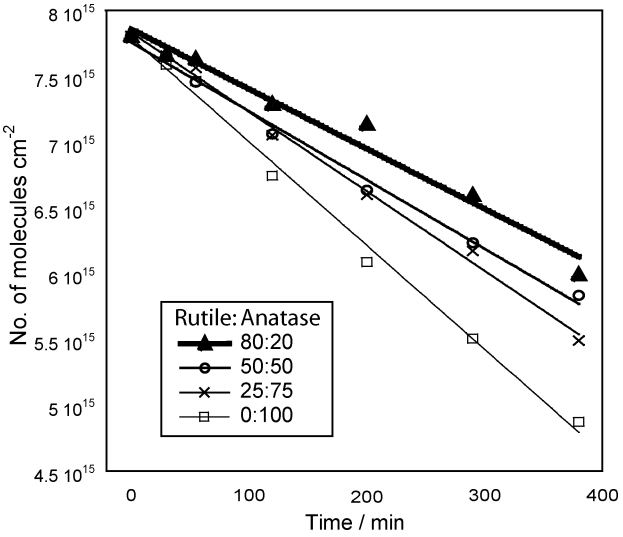

Figure 11. Plot of the number of molecules of stearic acid remaining on sections of the 600 °C film against UV irradiation time, showing the different rates of degradation.

morphology, we would expect the high rutile content spots to be the most photoactive. As this is not the case and in fact the reverse is observed, with the spots with the greatest anatase content having the highest photocatalytic activity, it is further confirmation that it is the nature of the phases present that is dominating the observed differences in photoactivity, and not the surface morphology.

The analysis of the film grown at 600 °C showed that it was composed of a mixture of the anatase and rutile phases of TiO_2. Effectively, we have been able to analyze the results of a combinatorial process where subtly changing reaction conditions at each spot (temperature, reactant concentration) have led to differing products and ratios of products. As the rutile in the film was only found 8 cm from the reactor entrance onward, this suggests that temperature is one of the key factors determining the formation of rutile in the film, as the reactant gas stream enters the reactor with a temperature between 200 and 250 °C, and will increase in temperature as it progresses through the much hotter reactor environment (600 °C).

Previous literature reports have found that photocatalytic activity is higher in TiO_2 films composed of anatase as compared to those composed of rutile,[18] when deposited in nanocrystalline films (i.e., by CVD). These results have been confirmed by the work in this paper where the most photoactive section of the investigated film was that composed only of the anatase phase. In these previous reports, however, only phase pure rutile and phase pure anatase were tested, while the combined film we have synthesized allows the mixed anatase/rutile systems to be investigated. This is significant because, although nanocrystalline films of anatase are used for self-cleaning coatings, they are not the most photoactive TiO_2 films that have been found, but are used as a compromise between optical clarity and photoactivity. The most effective coatings for optimizing photoactivity alone are those made by deposition of macroparticulate TiO_2, specifically Degussa P25, a 20% rutile to 80% anatase mixture.[26] The reason such macroparticles are more effective photocatalysts is believed to be because, somewhat counter-intuitively, they have a higher surface area (per unit film area) than the smoother nanocrystalline coatings.[16] Thus,

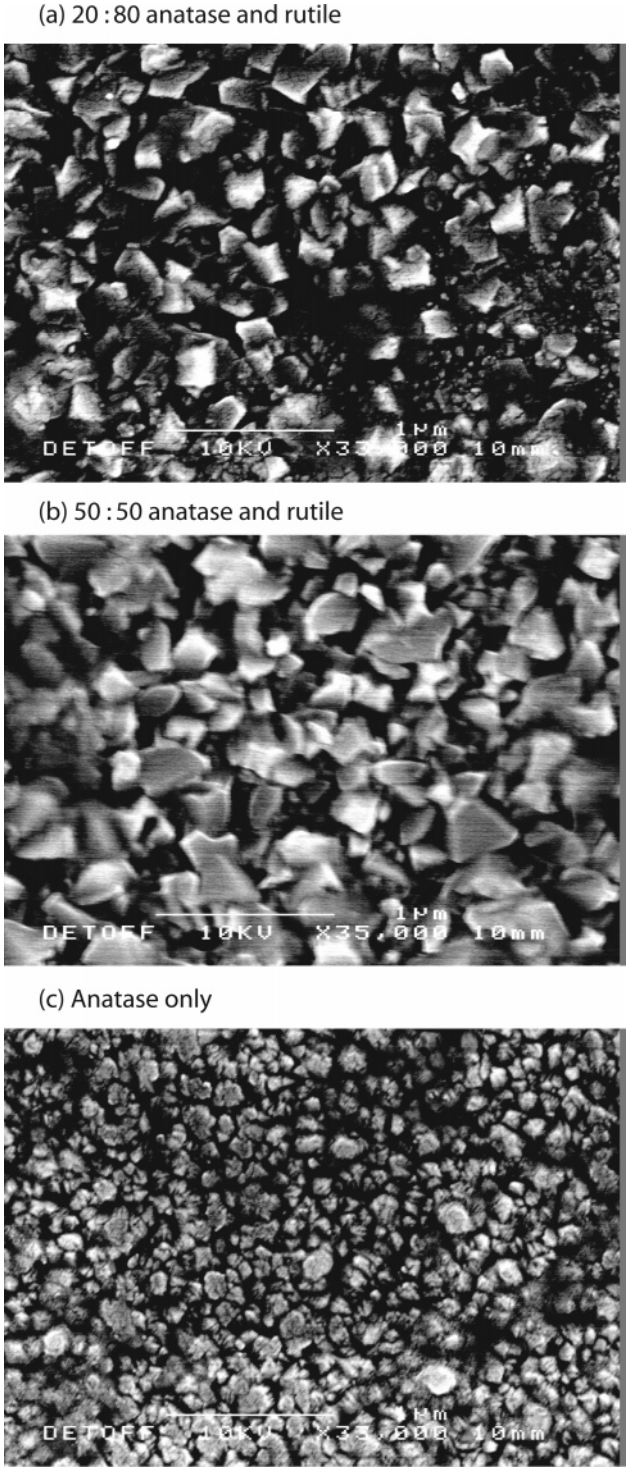

Figure 12. SEM images of various spots of the 600 °C film of anatase: rutile of: (a) 20:80, 33 000× magnification; (b) 50:50, 35 000× magnification; and (c) 100:0, 33 000× magnification.

our film containing a range of rutile:anatase ratios has allowed us to test the photoactivity of a 25:75 ratio spot, very close to the ratio found in the superior Degussa 25-based films. As we find that in our nanocrystalline films the pure anatase film is still the more effective photocatalyst, and not the 25:75 rutile: anatase ratio, we can support the view that it is the particulate nature of Degussa P25 films that plays the more significant role in their effectiveness and not the specific ratio of phases.

Conclusion

In this paper, the efficacy of an X-ray diffraction mapping strategy to reveal changes in both preferred orientation and phase composition in TiO_2 thin films has been shown. Such mapping allowed the spots that were most likely to have property differences to be identified and on which the physical property measurements were carried out.

The investigation of the TiO_2 films found preferred orientation differences in the film deposited at 450 °C, although the physical properties did not seem to be dependent on them, but instead on the film thickness. The 600 °C film, however, did show a correlation between the observed phase changes and the physical properties; the photocatalytic and photoinduced superhydrophilicity was greatest where anatase was the predominant phase of titania present in the film.

Had both of the films been analyzed using X-ray diffraction at only a small number of points, or at a single point, rather than with the mapping strategy, much of the significant variation that we have found in the films would not have been apparent. It is therefore proposed that the X-ray mapping method described here and demonstrated with the TiO_2 films could be usefully applied to provide a more detailed analysis of other thin film systems in the future.

Experimental Methods

Reactor Setup and Conditions. Films of titania were deposited using a cold-wall atmospheric pressure CVD reactor made of a cylindrical silica tube, and with a graphite block inserted to act as the reactor bed and onto which the glass slides were placed. A top guide plate was used to limit the reactant gas flow vertically to a few centimeters through the center of the reactor. As the reactor was cold walled, the substrate was heated through the graphite block, which contained three Whatman heater cartridges.

The transport gas (N_2) was supplied to the system from a cylinder, and then divided into three lines, with the flow rate of each being independently controlled. All of the lines passed through a furnace set at 200 °C to preheat the gas, and two then passed through the precursor vapors in bubblers, before rejoining the third plain line in a mixing chamber. The combined gas stream from the mixing chamber then passed through a brass manifold containing several baffles to produce a wide laminar flow of gas into the reactor.

The two precursors used for the deposition were $TiCl_4$ (Aldrich 99.9%), the titanium source, and ethlyl-acetate (BDH, GPR grade), the oxide source. These precursors were introduced to the gas stream by vaporizing them in heated bubblers and transporting the vapor with the nitrogen passed through the bubbler. The full details of the reactor and gas flow setup have been previously published.[28]

The deposition was carried out on slides of standard Pilkington float glass of dimensions 89 × 225 × 4 mm^3 (width, length, thickness), precoated on one side with SiO_2. The films were deposited onto the SiO_2-coated side of the glass, which acts as a barrier layer to prevent ions diffusing from the glass into the film. Two films were made, the first using a substrate temperature of 450 °C, the second using a temperature of 600 °C. In both cases, the precursor flow rates were identical: the $TiCl_4$ bubbler was heated to 70 °C with a nitrogen flow of 0.5 L min^{-1}, while the ethyl-acetate bubbler was heated to 40 °C with a gas flow of 0.5 L min^{-1}; the plain line gas flow was 7.5 L min^{-1}. In both cases, the heated glass substrate was exposed to the combined, vapor-containing gas stream for 60 s. All N_2 gas used was 99.99% as supplied by BOC Gases.

(28) Price, L. S.; Parkin, I. P.; Hardy, A. M. E.; Clark, R. J. H.; Hibbert, T. G.; Molloy, K. C. *Chem. Mater.* **1999**, *11*, 1792−1799.

X-ray Diffraction Analysis. The resulting thin films of titania were analyzed using glancing angle powder X-ray diffraction (incident beam angle of 5°) in a Bruker-Axs D8 (GADDS) diffractometer. This instrument utilizes a large 2D area X-ray detector to record large sections of multiple Debye−Scherrer cones simultaneously; 34° in both θ and ω can be measured with 0.01° resolution without moving the detector. After collection, the data across the Debye−Scherrer cones can be integrated across ω to produce a standard one-dimensional, 2θ against intensity plot. The instrument utilizes a Cu X-ray source, monochromated ($K\alpha_1$ and $K\alpha_2$) using a gobbel mirror and collimated such that only a small area of the sample (approximately 3−4 mm^2) is illuminated by the beam at any one time. Despite the small sample illumination, diffraction patterns with acceptable signal-to-noise ratios can still be recorded in very short time-frames (2−10 min) due to the large amount of data that the area detector can collect simultaneously. The sample itself is placed on a flat stage that is motorized to automatically move in *x*, *y*, and *z* directions.

This combination of abilities (small illumination area, fast collection times, and moveable sample stage) makes the diffractometer ideal for recording the diffraction patterns of multiple "spots" across the surface of the thin film, that is, "mapping" the diffraction pattern (and therefore crystalline phase) changes across the surface.

To produce such X-ray diffraction maps, diffraction patterns were recorded across the surface of the titania films every centimeter in both the *x* and the *y* directions using a single frame (recording a diffraction pattern without moving the source or detector) with a collection time of 10 min and covering $20° < 2\theta < 54°$.

Other Analytical Methods. In this test, a 1 μL drop of water was placed on the film, and the diameter of the resulting drop was measured. This was then converted into the contact angle, the angle between a tangent from the droplet and the film surface at the point where they meet. A more hydrophobic film has a higher contact angle.

The photocatalytic ability of the films was determined by irradiating them with 254 nm UV light and measuring the rate of decomposition of a layer of deposited stearic acid.[24,26] The layer of stearic acid was deposited on the films by spin coating, placing a drop of 0.02 M stearic acid in methanol on the surface and then spinning the substrate in a centrifuge, evaporating the methanol, and leaving a film of stearic acid. The film was then irradiated with a single 8 W UV light, and the quantity of stearic acid remaining on the film was periodically checked by recording an IR spectrum (using a Shimadzu FT-IR 8700 spectrometer) over the range 3000−2750 cm^{-1}, where the C−H stretches for stearic acid are found (2922 and 2850 cm^{-1}). The integrated area of these peaks can then be converted into a value for the number of molecules of stearic acid present on the film. Previous work[24] has found that an integrated area of 1 cm^{-1} over the range corresponds to 3.17×10^{15} molecules cm^{-2}.

UV−vis spectroscopy was achieved using a Shimadzu UV-2401PC spectrometer, while Raman spectroscopy was conducted on a Renishaw inVia Raman microscope.

Acknowledgment. We would like to thank Mr. Kevin Reeve for his help with the SEM measurements and Dr. Steve Firth for advising on the Raman spectroscopy. I.P.P. thanks the Royal Society/Wolfson Trust for a merit award. EPSRC are thanked for financial support.

Supporting Information Available: Figures showing all diffraction patterns in strips A−H for films formed at both 450 and 600 °C. This material is available free of charge via the Internet at http://pubs.acs.org.

JA062766Q